COMPUTATIONAL MODELING OF A SUBMERGED PLATE WAVE ENERGY CONVERTER

Flávio Medeiros Seibt, fseibt@gmail.com
Programa de Pós-Graduação em Engenharia Oceânica (PPGEO) – Escola de Engenharia (EE) – Universidade Federal do Rio Grande (FURG) – Avenida Itália, km 8 – Rio Grande-RS

Eduardo Costa Couto, e.c.couto@uol.com.br
Paulo Roberto de Freitas Teixeira, pauloteixeira@furg.br
Elizaldo Domingues dos Santos, elizaldosantos@furg.br
Liércio André Isoldi, liercioisoldi@furg.br
Programa de Pós-Graduação em Engenharia Oceânica (PPGEO) – Programa de Pós-Graduação em Modelagem Computacional (PPGMC) – Escola de Engenharia (EE) – Universidade Federal do Rio Grande (FURG) – Avenida Itália, km 8 – Rio Grande-RS

Luiz Alberto Oliveira Rocha, luizrocha@mecanica.ufrgs.br
Programa de Pós-Graduação em Engenharia Mecânica (PROMEC) – Universidade Federal do Rio Grande do Sul (UFRGS) - Rua Sarmento Leite, 425 - 2º Andar – Porto Alegre- RS

Abstract*. The need for clean and renewable energy sources has contributed to give relevance to the study of sea wave energy nowadays. This paper presents a computational model developed to analyze a submerged plate wave energy converter that transforms sea wave energy into electric energy. The basic principle of this device consists in the passage of sea waves through a horizontal submerged plate, generating a flow under it, where a Wells type turbine is placed and converts mechanical energy into electric energy. The model uses the commercial codes "GAMBIT" and "FLUENT". In the latter, the methodology used to represent the air-water interaction in the numerical simulations of the device is the multiphase volume of fluid (VOF) method. The objective of this paper is to analyze the influence of the distance from the plate to the bottom of the sea in the efficiency of the converter. To do so, the model, after a validation process, was used in six simulations that differ from each other only in the vertical position of the plate in a wave tank. The simulation showed that 5% increase in the distance from the plate to the bottom may produce 85% increase in the efficiency of the plate.*

Keywords*: submerged plate, wave energy, ocean waves, sea waves, FLUENT*

1. INTRODUCTION

The damage caused to the environment by the burning of fossil fuels and the elevated cost due to the continuous search for new reserves have encouraged the interest in clean and renewable energy sources. The ocean energy is one of the main renewable resources of the planet. The portion of ocean energy that is associated to the movement of water particles which occur in the surface of the waves or under it, is called wave energy.

Unlike wind energy, there are several technologies for the conversion of wave energy into electric energy. Different criteria are used to classify these converters. The most usual criteria are their position regarding the surface of the ocean, the distance from the coast line and the power take off or the energy conversion principles. According to the last criterion the converters are classified as follows: oscillating water column, floating bodies and over-topping (CRUZ;SARMENTO, 2004). Nowadays, none of the mentioned devices are in a leading position from the commercial point of view and the different wave energy conversion principles are expected to be used according to the characteristics of the location of the converter (CHOZAS;SOERENSEN, 2009).

The submerged plate is a structure commonly used in coastal engineering as a breakwater or a wave energy converter. There is little research about this type of converter; Orer and Ozdamar's experimental work (2007) has presented promising results.

The working principle of the submerged plate type converter, shown in Fig. 1, consists in the transformation of the mechanical energy in the flow that occurs under a submerged horizontal plate into electrical energy through a Wells type turbine due to the incidence of waves.

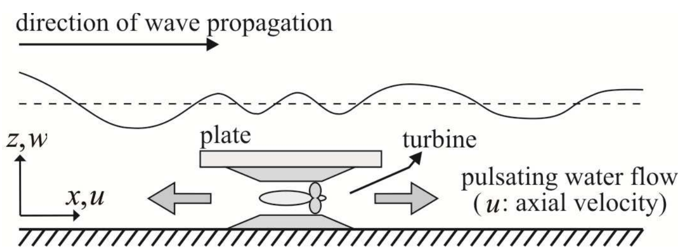

Figure 1. The working principle of the submerged plate type converter.

The Wells type turbine maintains the same direction of rotation regardless of the flow direction. In the submerged plate type converters, this characteristic is particularly well-applied because the flow under the plate change directions.

This paper reports a numerical analysis that relates the vertical position of the plate with associated variables to the efficiency of the device. In order to do so, initially the methodology was validated and then, six situations - that differ from each other only by the vertical position of the plate - were analyzed. In this paper, the influence of the turbine on the flow was disregarded.

2. NUMERICAL MODEL AND SIMULATION CONDITIONS

A submerged horizontal plate positioned in a middle of a tank is the numerical domain used to the study cases, as shown schematically in Fig. 2. The computational model that analyzes the submerged plate type converter uses the commercial codes GAMBIT and FLUENT. The first one was used for the discretization of the domain through the construction of structured meshes with quadrilateral elements. The other one discretizes the differential equations of conservation and transport and solves the algebraic system of equations.

The Volume of Fluid (VOF) method was used to consider both water and air phases. The PRESTO! method was used as an upwind advection scheme for the space pressure discretization, while the Geo-reconstruction method was used for the interface reconstruction of the fluids. The PISO algorithm (Pressure-Implicit with Splitting of Operator) was used as a pressure-velocity coupling method. Sub-relaxation factors of 0.3 and 0.7 were used for mass conservation and momentum equations, respectively.

The boundary conditions were: atmospheric pressure on the upper side of the tank; time-dependent velocity on the left side of the tank up to the free surface level and a condition of no slip on the other surfaces (Figure 2). Time-dependent velocity in the x and z directions used as a boundary condition on the left side of the tank is obtained from the second order Stokes wave theory and are defined by the Eqs. (1) and (2) (CHAKRABARTI, 2005), respectively:

$$u(x,z,t) = \frac{\pi H}{T}\frac{\cosh k(h+z)}{\sinh kh}\cos(kx-\sigma t) + \frac{3}{4}\frac{(\pi H)^2}{TL}\frac{\cosh 2k(h+z)}{\sinh^4 kh}\cos 2(kx-\sigma t) \tag{1}$$

$$w(x,z,t) = \frac{\pi H}{T}\frac{\sinh k(h+z)}{\sinh kh}\sin(kx-\sigma t) + \frac{3}{4}\frac{(\pi H)^2}{TL}\frac{\sinh 2k(h+z)}{\sinh^4 kh}\sin 2(kx-\sigma t) \tag{2}$$

where H is the wave height, h is the depth, x is the position, t represents the time, and z is the position in relation to free surface average level. $k = 2\pi / L$ and $\sigma = 2\pi / T$ are the wave number and the wave angular frequency, respectively, L is the wave length and T the wave period.

The methodology used in the model is summarized in Table 1.

Table 1. Model methodology.

Formulation	Method
Solution in time	Transient Implicit formulation of 1st order Pressure based Non iterative advance in time
VOF Model	Explicit formulation
Solution control	Pressure-velocity coupling method: PISO Pressure discretization method: PRESTO! Momentum formulation method: *Upwind* of 1st order Geometric fraction discretization scheme: *Geo-reconstruct*

3. VERIFICATION AND VALIDATION OF THE COMPUTER MODEL

The wave tank used in the simulations, shown in Fig. 2, has the same characteristics as the ones used by Orer and Ozdamar (2007) in the experiments that evaluate the effectiveness of the submerged plate device. In this figure, H_p is the plate height that represents the distance between the bottom and the plate. This study analyses the effects of H_p distance on the converter efficiency.

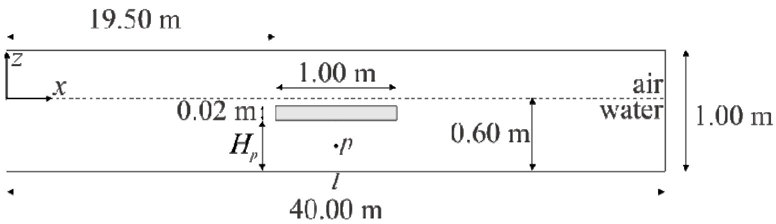

Figure 2. Geometry of the tank and the plate.

All simulations were carried out until 40s using a time step equal to 0.001s. The processing time of each case, corresponding to 40 s of monitoring, was approximately 20 hours in a computer with an Intel Core 2 Quad of 2.66 GHz processor working with four active cores. Initially, a mesh independence study was carried out to choose the mesh to be used in the validation process and in the following simulations. After this study, the wave elevation and the velocity profiles numerically generated were compared with the analytical solution by using second order Stokes theory. After this comparison, the model under study was validated comparing numerical and experimental results.

3.1 Mesh independence study

In this study, the wave height (H) and the wave period (T) are equal to 0.06 m and 1.50 s, respectively, and the wavelength is 3.00 m, according to the linear theory. For H_p equal to 0.52 m, four simulations with the structured meshes described in Table 2 were carried out. During these simulations the mass flow which crosses a numerical gauge located under the plate (line l – Fig. 2) at instant t= 20 s was monitored. Based on the relative error in Table 2, mesh 3 was chosen for the following simulations since mesh 4 has a very similar error, even when volumes with 50% smaller characteristic dimensions are used.

Table 2. Mesh study (results obtained for the mass flow in $x = 20.00$ m at instant $t = 20$ s).

Mesh	Volume sizes (m)	Number of volumes	Mass flow (kg/s)	Relative error (%) between (j) and (j-1) results
1	0.04 × 0.04	12475	-34.85	–
2	0.02 × 0.02	49950	-31.71	9.02
3	0.01 × 0.01	399800	-31.37	1.09
4	0.005 × 0.005	799200	-31.67	0.98

3.2 Verification

For this comparison, similar to what has ocurred in the mesh independence study, the wave height (H) and the wave period (T) are 0.06 m and 1.50 s, respectively. For these wave characteristics and the canal depth equal to 0.60 m, the best theory to model the wave is the second order Stokes theory, according to Chakrabarti (2005).

In order to evaluate the model light of this theory firstly, numerical result and the analytical solution were compared in terms of time series of the free surface elevation. The latter was obtained from Eq. 3 (CHAKRABARTI, 2005).

$$\eta = \frac{H}{2}\cos(kx - \sigma t) + \frac{\pi H^2}{8L}\frac{\cosh 2h}{\sinh^3 kh}(2 + \cosh 2kh)\cos 2(kx - \sigma t) \tag{3}$$

In Fig. 3 there are numerical and analytical results of the free surface elevation for the position x =5 m. The mean squared difference between numerical and analytical results is equal to 2.55 % corresponding to a range of seven wave periods starting after the stabilization and finishing before the reflection due to the end wall of the canal. There are two reasons that show the good capacity of the model to simulate wave propagation: the small average error and the fact that the curves are in phase.

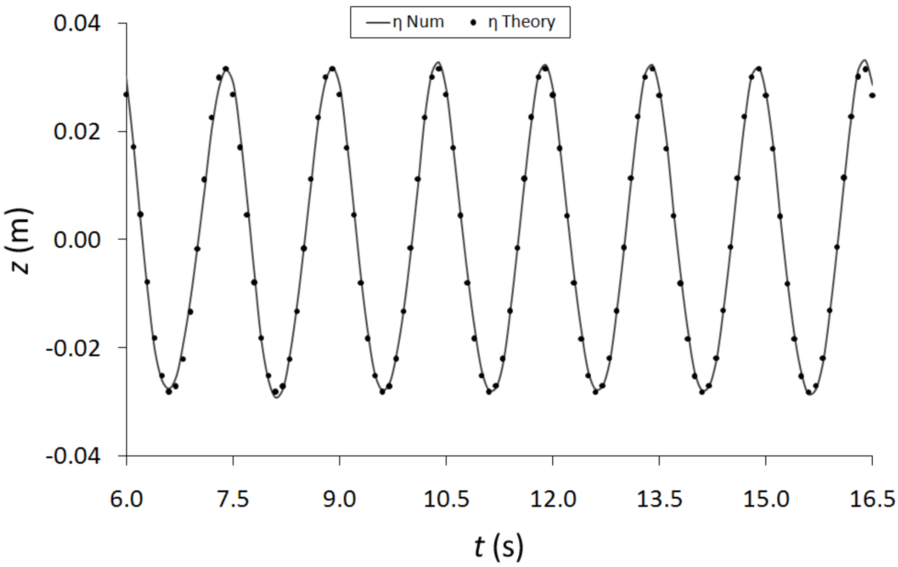

Figure 3. Comparison between numerical model and the second order Stokes theory.

To complement the numerical model evaluation according to the second order Stokes theory, the velocity profiles numerically obtained were compared with the analytical solution (CHAKRABARTI, 2005). Equations (1) and (2) correspond to analytical solutions for u and w velocity components in the x and the z directions, respectively. Figures 4 (a) and (b) show the four most representative profiles in the velocity field under the wave crest (Cr), the upward zero-crossing (Uz), the trough (Tr), the downward zero-crossing (Dz). Although some differences can be seen in zero-crossing wave positions, in general numerical profiles presented good agreement with those obtained analytically. These results confirm the model capacity to simulate the wave propagation phenomena.

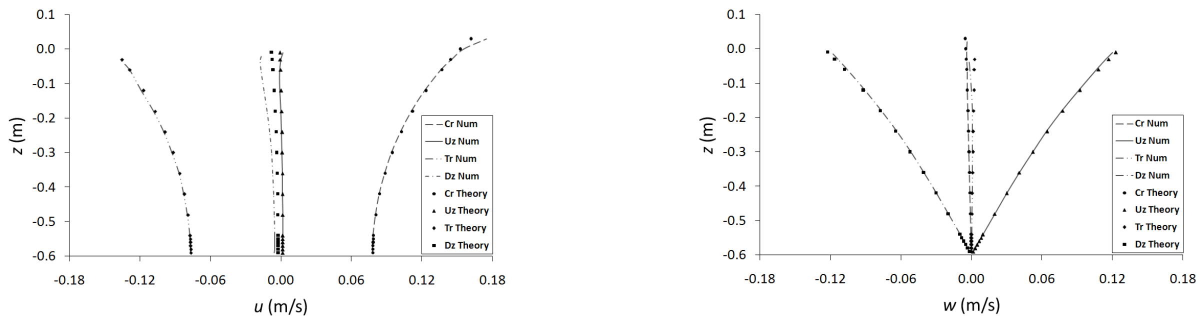

(a) (b)

Figure 4. Numerical versus analytical results (second order Stokes theory) for velocity components u and w .

3.3 Validation

Orer and Ozdamar (2007) carried out an experimental study aiming to determine the efficiency of the submerged plate wave energy converter. This study was developed in a wave tank shown in Fig. 2, whose plate height (H_p) was equal to 0.52 m. This experimental study aimed to measure the maximum velocities of the flow under the plate in the opposite direction of the wave propagation and to calculate the converter efficiency. The velocity measurements were carried out in a p point located in a mid position between the bottom and the plate, right at the center of the plate.

The maximum velocity measured in the experiments and the ones found by the numerical simulations were compared aiming to validate the model. Two experiments were selected from Orer and Ozdamar's analysis (2007) to make the comparisons. The simulations were carried out with a structured mesh formed by 399800 squared elements with the side equal to 0.01 m according to the mesh independence study.

The wave parameters of each experiment, the velocity and the relative differences are presented in Table 3. The wave of the first experiment has the same parameters as the one used in the mesh independence and the verification procedures. The Japanese equipment (Kenek) Vm-801 H model (ORER; OZDAMAR, 2007) was used to measure the velocities. This instrument has $\pm 2\%$ accuracy along the range [0, $\pm$200] cm/s (KENEK, 2012). The measurement uncertainty depends on the series of instruments that compose the measurement system. It is observed that the relative differences between numerical and experimental results were around 11 %.

Table 3. Wave parameters, experimental and numerical results and relative differences.

Wave	*T* (s)	*H* (m)	Experimental result (cm/s)	Numerical result (cm/s)	Relative difference (%)
1	1.50	0.06	-9.44	-8.34	11.67
2	1.87	0.06	-11.39	-12.72	-11.74

4. RESULTS

After the mesh independency study and the verification and the validation procedures of the computer model, the influence of the plate height (H_p) in its efficiency as a converter device of the wave energy was studied by six simulations, considering the same wave characteristics adopted for the verification process. This study identified the variation of the device efficiency and some parameters associated with availability of energy to be captured by a Wells turbine. Besides the efficiency, the parameters under evaluation were: the maximum velocity flow and the average mass flow under the plate.

In the six cases under study the plate heights (H_p) are: 0.46 m, 0.48 m, 0.50 m, 0.51 m, 0.52 m and 0.53 m. In each case, the velocities were measured at several points (Fig. 5) distributed between the bottom and the middle of the plate. The mass flow under the plate to each time step of 0.001s for further calculation of its squared average was also measured. For the efficiency calculation, the dynamic pressure (DEAN; DALRYMPLE, 1991) was measured at the same points where the velocities were measured. The following results correspond to the same interval of time used in the validation process. Fig. 5 shows the maximum velocity profiles in the direction of the wave propagation and in the opposite direction for the six study cases.

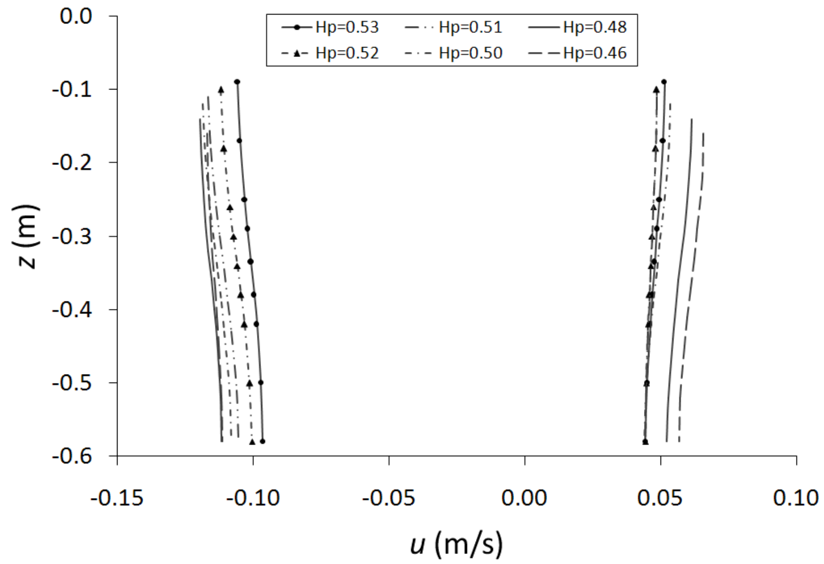

Figure 5. Maximum velocity profiles: the same wave propagation direction and the opposite direction.

It is noteworthy that the highest velocities occur in the opposite direction of the wave propagation and the decrease of the plate height produces an important reduction in the velocities without changing significantly their profiles. Figure 6 presents the maximum velocities for each case. The occurrence of a minimum value is observed for the height of 0.48 m. To the left and to the right of this value there are similar curve slopes. Up to 0.51 m, the slope increases approximately five times.

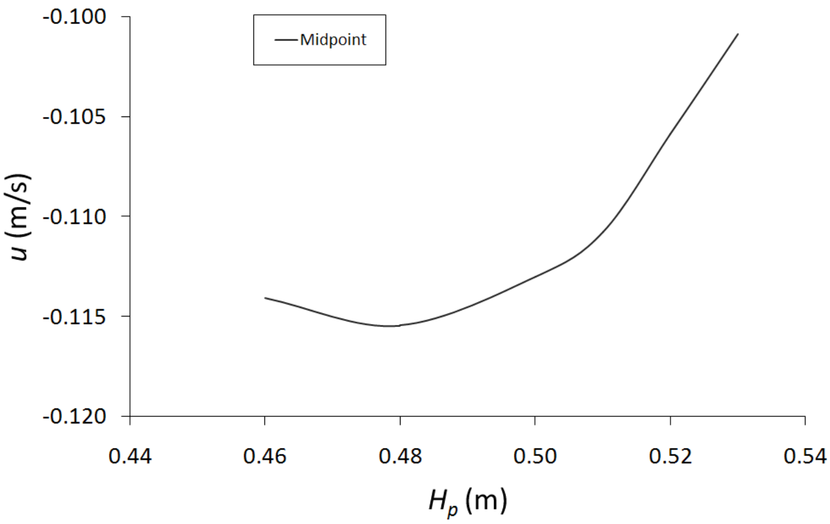

Figure 6. Maximum velocity flow under the plate in each case.

The Root mean square (RMS) mass flow under the plate for each case is shown in Fig. 7. The more the plate height increase, the more its value goes up. The heights 0.48 m and 0.52 m divide the curve into three parts. The end parts have a steeper slope in relation to the intermediate one.

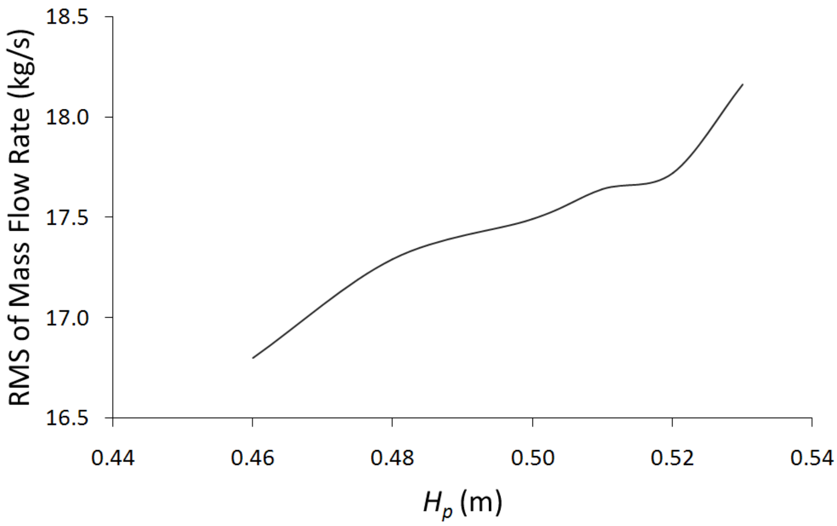

Figure 7. Root mean square (RMS) of the mass flow under the plate for each case.

The device efficiency can be calculated by the expression proposed by Graw (1995):

$$\varphi = \frac{\text{available power under the plate}}{\text{wave power}} = \frac{P_p}{P_w} \tag{4}$$

where P_w is the wave power that acts on the device; it is obtained from the expression proposed by Dean and Dalrymple (1991),

$$P_w = \left(\frac{1}{8}\rho g H^2\right)\frac{\sigma}{k}\left[1 + \frac{2kh}{\sinh 2kh}\right] \tag{5}$$

and P_p, the available power under the plate, is calculated in a similar way to the one proposed by Dizadji and Sajadian (2011),

$$P_p = \frac{1}{T}\int_t^{t+T}\int_{-h}^{-h+H_p}\left(P_D + \frac{1}{2}\rho u^2\right) u \, dz \, dt \tag{6}$$

where P_D is the dynamic pressure.

Figure 8 shows the device efficiency values in relation to the heights. In this figure, the curve has a minimum value when the plate height is equal to 0.50 m. It can be noticed that the curve has a slope on the left side of the minimum value six times lower than that on the another side. Similar growth is also observed in the behavior of the maximum velocity and the square mean of the mass flows (Fig. 6 and 7). These results show that the increase of height around 5% can also increase the device efficiency up to approximately 86 %.

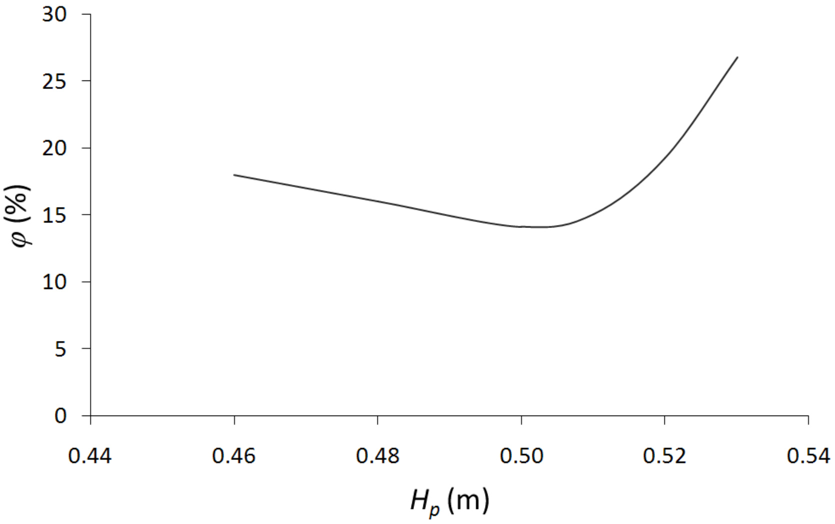

Figure 8. Efficiency of the submerged plate wave energy converter for different plate heights.

5. CONCLUSIONS

This paper reports a study that analyzed the efficiency of the submerged plate numerically as a wave energy converter device. The maximum velocity of the flow and mean mass flow under the plate and the device efficiency were calculated by varying the plate height. The simulations showed that the increase in the plate height do not always lead to the maximum velocity reduction. However, the increase of the plate height and, consequently, increase of the transversal flow area under the plate always results in an increase in the mass flow under the plate. Finally, this paper presented the variation of the device efficiency with the plate height, showing the importance of the plate position. It was observed that up to the minimum height of 0.50m, the increase of height around 5% can also increase the device efficiency up to approximately 86%. Other studies have been developed to investigate the influence of the turbine and the plate length in the device efficiency.

6. REFERENCES

Chakrabarti, S. K., 2005. Handbook of Offshore Engineering. Elsevier, Plainfield.

Chozas, J. F. and Soerensen, H. C., 2009. State of the art of wave energy in Spain, Proc. 3rd Annual Electrical Power and Energy Conference (EPEC), Montreal, QC, Canada, IEEE, 1-6.

Cruz, J. M. B. P. and Sarmento, A. J. N. A., 2004. Energia das ondas: Introdução aos aspectos tecnológicos, econômicos e ambientais, Instituto do Ambiente, 65p.

Dean, R. G. and Dalrymple, R. A., 1991. Water Wave Mechanics for Engineers and Scientists, World Scientific Publishing Co. Pte. Ltd., 355p.

Dizadji, N. and Sajadian, S. E., 2011. Modeling and optimization of the chamber of OWC system, Energy, 36 (5), 2360-2366.

Graw, K. U., 1995. Wellenenergie – eine hydromechanische Analyse, Bericht Nr. 8 des Lehr- und Forschungsgebietes Wasserbau und Wasserwirtschaft, Bergische Universitaet – Gesamthochschule, Wuppertal, Germany, 332p.

Kenek, Electromagnetic Current Meter. Retrieved March 15, 2012, from http://www.hangilco.com/VM-801.htm.

Orer, G.; Ozdamar, A., 2007. " An experimental study on the efficiency of the submerged plate wave energy converter". Renewable Energy, n. 32, p.1317–1327.

6. RESPONSIBILITY NOTICE

The authors are the only responsible for the printed material included in this paper.